

CHEMISTRY

A European Journal



Accepted Article

Title: Towards an improved design of MRI Contrast Agents: Synthesis and Relaxometric Characterisation of Gd-HPDO3A Analogues

Authors: Louise Rachel Tear, Carla Carrera, Eliana Gianolio, and Silvio Aime

This manuscript has been accepted after peer review and appears as an Accepted Article online prior to editing, proofing, and formal publication of the final Version of Record (VoR). This work is currently citable by using the Digital Object Identifier (DOI) given below. The VoR will be published online in Early View as soon as possible and may be different to this Accepted Article as a result of editing. Readers should obtain the VoR from the journal website shown below when it is published to ensure accuracy of information. The authors are responsible for the content of this Accepted Article.

To be cited as: *Chem. Eur. J.* 10.1002/chem.202000479

Link to VoR: <http://dx.doi.org/10.1002/chem.202000479>

Supported by
ACES

WILEY-VCH

FULL PAPER

Towards an improved design of MRI Contrast Agents: Synthesis and Relaxometric Characterisation of Gd-HPDO3A Analogues

Louise R. Tear,^[a] Carla Carrera,^[b] Eliana Gianolio,^{*,[a]} and Silvio Aime^{*,[a]}

[a] Dr. L.R. Tear, Dr. E. Gianolio and Prof. S. Aime
Department of Molecular Biotechnology and Health Sciences
Molecular Imaging Centre, University of Torino
Via Nizza 52, 10126 Torino, Italy
E-mail: eliana.gianolio@unito.it

[b] Institute of Biostructures and Bioimaging, National Research Council, Turin, Italy

Supporting information for this article is given via a link at the end of the document.

Abstract: The properties of Ln(III)-HPDO3A complexes as relaxation enhancers and paraCEST agents are essentially related to the hydroxypropyl moiety. A series of three HPDO3A derivatives, with small modifications to the hydroxyl arm, were herein investigated to understand how heightened control can be gained over the parameters involved in the design of these agents. A full ¹H and ¹⁷O-NMR relaxometric analysis was conducted and demonstrated that increasing the length of the OH group from the lanthanide centre significantly enhanced the water exchange rate of the gadolinium complex, but with a subsequent reduction in kinetic stability. Alternatively, the introduction of an additional methyl group, which increased the steric bulk around the OH moiety, resulted in formation of almost exclusively the TSAP isomer (95 %) as identified by ¹H-NMR of the europium complex. The gadolinium analogue of this complex also exhibited a very fast water exchange rate, but with no detectable loss of kinetic stability. This complex therefore demonstrates a notable improvement over Gd-HPDO3A.

Introduction

Contrast agents are widely used in magnetic resonance imaging (MRI) to enhance the differentiation and characterisation of pathological tissue.^[1] One of the contrast agents most commonly applied in clinical practice is Gd-HPDO3A (Prohance, Bracco), which was first reported almost 30 years ago.^[2] In recent years there has been concern regarding the discovery of Gd deposition in the brain and other tissues of patients, after contrast-enhanced MRI scans.^[3–6] Gd-HPDO3A appears to be one of the agents which displays a lower level of retention in the body than most other Gd contrast agents,^[7–9] in part due to its high kinetic stability as a macrocyclic agent.^[10,11] The relaxometric properties of Gd-HPDO3A have been investigated extensively.^[12] These studies suggest that while the prototropic exchange of the OH group significantly enhances the relaxivity of the complex, this effect may only contribute at basic pH. However, it has been determined that the OH-proton has a shorter Gd-H distance than Gd-H₂O and therefore T_{1M} of the hydroxyl proton is approximately 50 % shorter than that of the coordinated water protons.^[13,14] Studies have investigated extensively the solution structure of Ln-HPDO3A complexes, which have shown how the SAP to TSAP ratio changes along the lanthanide series.^[12] In Gd-HPDO3A the

ratio of SAP to TSAP isomers in aqueous solution is 70 % SAP to 30 % TSAP. TSAP isomers are known in general to display shorter water residency times (τ_m) than SAP isomers, due to the increased steric hindrance surrounding the coordinated water molecule. Therefore, the proportion of these two diastereoisomers affects the overall observed τ_M value.^[15] It has also been shown that the slow exchange rate of the hydroxyl proton allows the use of paramagnetic Ln-HPDO3A complexes as para-CEST agents.^[16] In particular, these complexes can act as ratiometric pH reporters due to the two CEST hydroxyl signals, which correspond to the SAP and TSAP isomers.^[17]

The overall properties of Gd-HPDO3A as relaxation enhancers and of Yb and Eu-HPDO3A as para-CEST agents are therefore essentially related to the occurrence of the hydroxypropyl moiety. This group affects the overall neutral charge of the complexes, their stability, the ratio of TSAP/SAP, the rate of water exchange etc., when compared to the parent DOTA complexes. On this basis we deemed it of interest to introduce chemical changes to the OH bearing arm to assess whether one may acquire heightened control of the parameters involved in the design of relaxation enhancers or of para-CEST agents.

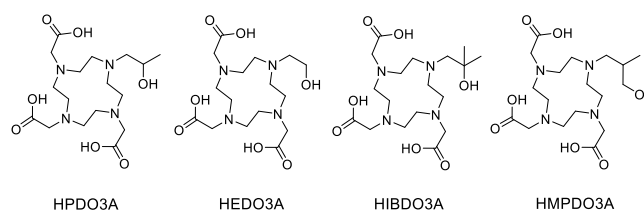


Figure 1. Structure of HPDO3A and derivatives: HEDO3A (10-(2-hydroxyethyl)-1,4,7,10-tetraazacyclododecane-1,4,7-triacetic), HIBDO3A (10-(2-hydroxyisobutyl)-1,4,7,10-tetraazacyclododecane-1,4,7-triacetic acid), HMPDO3A (10-(3-hydroxy-2-methylpropyl)-1,4,7,10-tetraazacyclododecane-1,4,7-triacetic acid).

Here, we report the results obtained by comparing the parent Gd-HPDO3A complex and three new derivatives (Figure 1). The ligands have been designed to alter the properties of the hydroxyl group through its structural environment. These involve either the addition or removal of a simple methyl group (HIBDO3A and HEDO3A respectively), or the elongation of the hydroxyl chain by

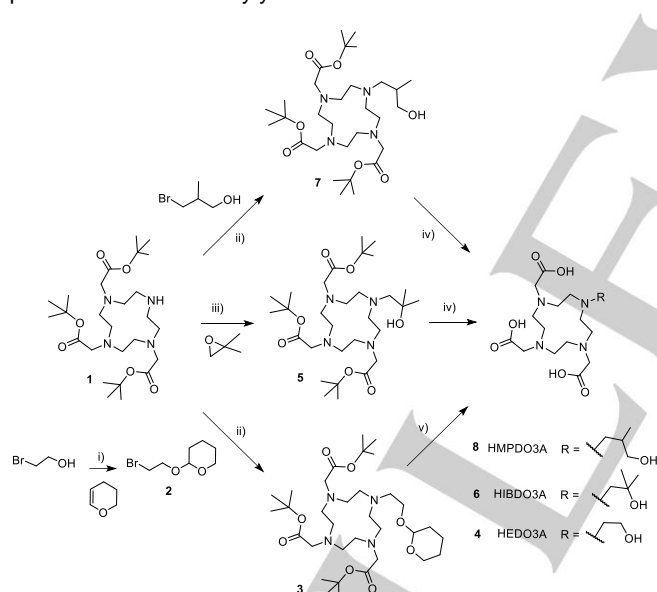
FULL PAPER

one carbon (HMPDO3A). A full relaxometric study of the Gd complexes has been carried out, including analysis of the SAP/TSAP ratio with high resolution $^1\text{H-NMR}$ of the Eu complexes and $^{17}\text{O-NMR}$ and NMRD of the Gd complexes. The new complexes have been thoroughly assessed to gain insight into the modulation of the properties of the Ln complex through the modifications introduced at the OH-bearing arm.

Results and Discussion

Synthesis

The HPDO3A derivatives were synthesised through the scheme shown in Scheme 1. The syntheses of all the ligands involved the alkylation of the protected triester **1** with the appropriate substituent to give intermediates **3**, **5** and **7**. In the case of **3**, 2-bromoethanol was protected with tetrahydropyran (**2**) prior to addition to **1**. The intermediates of the ligands were then deprotected by TFA and purified via chromatography on Amberchrom® to give the final ligands **4**, **6** and **8**. Triester **1** was synthesised according to literature procedures and used as the starting material for all three ligands.^[19] HEDO3A was previously synthesised in the literature with a different procedure, which involved the direct addition of 2-bromoethanol to DO3A (deprotected **1**).^[19] Our strategy allows an easier purification of the product with satisfactory yields.



Scheme 1. Synthesis of HPDO3A derivatives: i) pyridinium p-toluenesulfonate, DCM, 12 h, RT; ii) K_2CO_3 , ACN, 12 h, RT; iii) DIPEA, ACN, 48 h, 50 °C; iv) DCM, TFA then TFA with triisopropylsilane, 60 h, RT; v) water, THF, acetic acid, 24 h, RT then TFA with triisopropylsilane, 72 h, RT.

High resolution solution $^1\text{H-NMR}$

As Europium is one of the closest elements to Gadolinium it is customary to acquire the $^1\text{H-NMR}$ of the europium complexes in order to determine the ratio of isomers in aqueous solution (SI). Octa-coordinated, tetra-aza-cyclododecane based macrocyclic ligands are known to wrap around Lanthanide (III) ions to yield four isomers, namely two Square Anti-Prismatic (SAP) and two

Twisted Square Anti-Prismatic (TSAP) isomers, which depend on the torsion angle (δ or λ) of the macrocyclic ring and the orientation of the pendant arms (Δ or Λ). This leads to four possible diastereoisomers: $\Delta(\lambda\lambda\lambda)$ (SAP1), $\Lambda(\delta\delta\delta)$ (SAP2), $\Lambda(\lambda\lambda\lambda)$ (TSAP1) and $\Delta(\delta\delta\delta)$ (TSAP2). In addition to this, Ln-HMPDO3A (like Ln-HPDO3A) has a chiral carbon which can be either *R* or *S* and creates the possibility of a total of 8 isomers. Based on crystallography data of Gd-HPDO3A,^[13] the dominant diastereoisomers in solution of Eu-HPDO3A were assumed to be SAP2-*R* and TSAP1-*R* and their enantiomeric pairs SAP1-*S* and TSAP2-*S*.^[12]

It was early established that the axial ring proton region is highly diagnostic for assessing the SAP/TSAP isomeric ratio. These protons are highly shifted downfield in EuDOTA-type complexes (10 – 50 ppm), with the SAP isomer experiencing a greater chemical shift than the TSAP isomer protons. Figure 2 shows the axial region of Eu-HMPDO3A with assignment of the protons for each isomer. Interestingly, in respect to the parent Eu-HPDO3A complex and to the Eu-HIBDO3A and Eu-HEDO3A derivatives (see Supp. Info. Figures S10 and S13), an additional minor set of peaks in the SAP and TSAP region are present. These are most likely ascribable to the SAP1 and TSAP2 isomers, which in this case have a different chemical shift to those of SAP2 and TSAP1, as has previously been observed for Eu-HPDO3MA.^[20] In analogy with Eu-HPDO3A, the diastereoisomers of Eu-HMPDO3A can be assigned as SAP2-*R* (35 %), SAP1-*R* (15 %) and TSAP1-*R* (35 %), TSAP2-*R* (15 %), with their corresponding *S* enantiomers also present.

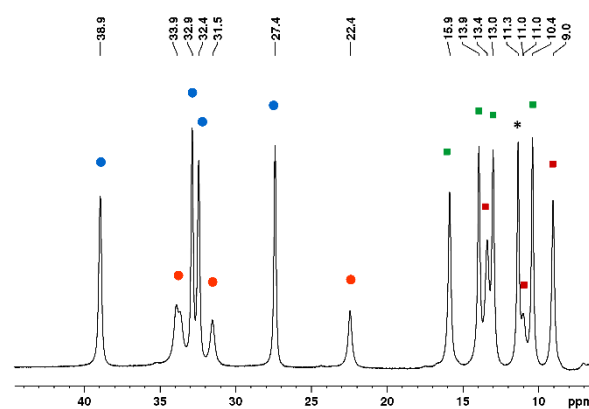


Figure 2. Axial region of $^1\text{H-NMR}$ of Eu-HMPDO3A in D_2O at pH 7.4, 600 MHz. Peaks labelled as follows: SAP2-*R*/1-*S* = blue, SAP1-*R*/2-*S* = orange, TSAP1-*R*/2-*S* = green, TSAP2-*R*/1-*S* = red. * peaks excluded from TSAP contribution based on EXSY information.

2D EXSY-NMR were acquired to identify the exchange between isomers and to aid the assignment of isomer peaks (SI). In Eu-HMPDO3A, the EXSY NMR (Figure 3) indicates ring inversion of the major SAP2-*R*/1-*S* and TSAP1-*R*/2-*S* isomers (box A) and one arm rotation between the minor SAP1-*R*/2-*S* protons and the major TSAP1-*R*/2-*S* protons (box B). With longer mixing time (10 ms instead of 5 ms, Figure S17) exchange via ring inversion of the minor SAP1-*R*/2-*S* isomer is also observable and indicates exchange to the same protons as the major TSAP1-*R*/2-*S* isomer. The other peaks in the TSAP axial region (red in Figure 2) have been assigned as the TSAP2-*R*/1-*S* minor isomer. These protons do not demonstrate exchange via arm rotation with that of the

FULL PAPER

SAP2-*R*/1-*S* major isomer, but there is evidence of ring inversion of both isomers, which indicates that arm rotation between these two isomers is most likely blocked.

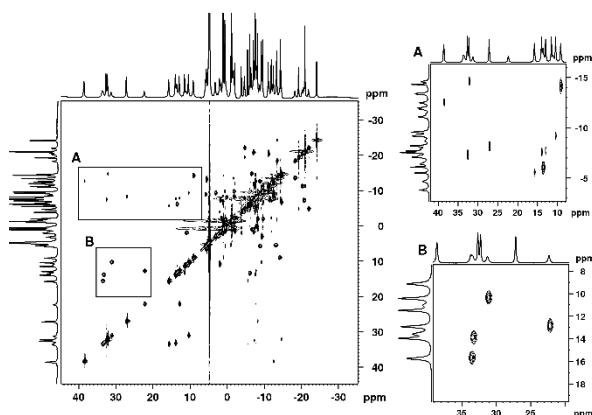


Figure 3. 2D EXSY $^1\text{H-NMR}$ of 100 mM EuHMPDO3A, with 5 ms mixing time in D_2O at pD 7.4, 275 K, 600 MHz. Cross peaks show the exchange between isomers by A) ring inversion and B) arm rotation.

The high resolution $^1\text{H-NMR}$ spectrum of Eu-HEDO3A in D_2O (Figure S10) indicates the presence of both SAP and TSAP isomers in a ratio of SAP 50 % and TSAP 50 %. The pairs of TSAP and SAP isomers are indistinguishable in the $^1\text{H-NMR}$, as with Eu-HPDO3A. The 2D EXSY spectrum (Figure S11) indicates proton exchange between the isomers via ring inversion and also via arm rotation. Each proton resonance in the axial region (SAP and TSAP) has three corresponding cross peaks, two which show exchange to equatorial protons and one to the axial protons of the alternate isomer (i.e. SAP_{ax} to TSAP_{ax}). The proton resonances which are linked by arm rotation (SAP_{ax} and TSAP_{ax}) exchange with the same set of equatorial protons through ring inversion. This indicates that all four isomers are populated, as previously observed for DOTA,^[21] and that the chemical shifts of SAP and TSAP diastereoisomers are almost equivalent and therefore appear together in the spectrum.

In contrast to the other complexes, the $^1\text{H-NMR}$ of Eu-HIBDO3A (Figure S13) shows almost only the TSAP isomer (95 %). TSAP most likely dominates due to the isobutyl group increasing the steric bulk around the bound metal, which limits isomerization and forces a specific conformation.^[22] This has been previously reported for chiral complexes,^[23,24] as well as for DOTMA and HPDO3MA,^[20,25] which display a high proportion of the TSAP isomer in part due to blocked isomer exchange. The very small quantity (5%) of SAP isomer present in the EXSY spectrum (Figure S14) demonstrates some proton exchange via arm rotation and ring inversion between the SAP and TSAP isomers in solution. It is therefore possible that both TSAP enantiomers are populated and there is exchange between these two (either by direct enantiomeric exchange, or via the SAP isomer which does not remain significantly populated). The proton resonances of TSAP1 and TSAP2 isomers would therefore occur with the same chemical shifts and the contribution of each to the 95 % observed is unknown.

Exchange of isomers via arm rotation was observable in the EXSY NMR of all three derivatives, but has not been observed in that of Eu-HPDO3A.^[12] This has previously been attributed to the

assumption that exchange by arm rotation is too fast to observe on the NMR timescale. However, in these derivatives, arm rotation of the less hindered Eu-HEDO3A and longer armed Eu-HMPDO3A, would be anticipated to be faster than that of Eu-HPDO3A. Therefore, it is possible that arm rotation is blocked in the parent compound and that only the two dominant diastereoisomers are populated (SAP2-*R*/1-*S*) and TSAP1-*R*/2-*S*).

All three derivatives also have an additional proton resonance in the TSAP axial region (* in Figure 2, S10 and S13), which has been excluded from the TSAP axial protons, due to the absence of corresponding cross peaks that would indicate arm rotation with the SAP isomer in the EXSY spectrum. In Figure 2, the proton resonances assigned to the TSAP2-*R*/1-*S* minor isomer (red) most likely also have an additional proton present, as indicated by the integrals of these regions. Eu-HPDO3A also displays this additional proton resonance within this region, while Eu-DOTA does not, therefore indicating it probably corresponds to one of the protons on the hydroxyl arm. A comparison of these three complexes with Eu-HPDO3A would suggest that the CH_2 group on the hydroxyl arm is the most likely candidate, as it is the only group which remains unchanged between all complexes.

The relative populations of each isomer were calculated by integration of the protons in the axial region and are displayed in Table 1.

Table 1. Percentage of SAP and TSAP isomers in europium and gadolinium complexes.

Ligand	Eu Complex ^[a]		Gd complex ^[b]	
	SAP %	TSAP %	SAP %	TSAP %
HPDO3A	60	40	70	30
HEDO3A	50	50	60	40
HIBDO3A	5	95	6	94
HMPDO3A	50 (35 – 2 <i>R</i> /1 <i>S</i> 15 – 1 <i>R</i> /2 <i>S</i>)	50 (35 – 1 <i>R</i> /2 <i>S</i> 15 – 2 <i>R</i> /1 <i>S</i>)	60	40

[a] From $^1\text{H-NMR}$ peak integrals at 275 K, 600 MHz. [b] Empirically extrapolated from Eu ratios using the equation: $\chi_{\text{SAP}}(\text{Gd}) = \chi_{\text{SAP}}(\text{Eu}) \times 1.16$; $\chi_{\text{TSAP}}(\text{Gd}) = 100 - \chi_{\text{SAP}}(\text{Gd})$

Relaxometric Analysis

It has been consistently reported that TSAP isomers display faster water exchange rates than those of SAP isomers. In general, the overall observed relaxivity is frequently limited by the relatively slow exchange rates due to a low proportion of the TSAP isomer. The proportion of TSAP and SAP isomers and their differing water exchange rate characterise the variable-temperature $^{17}\text{O-NMR}$ transverse relaxation rate profiles (R_2) and influence the amplitude of the NMRD profiles. Therefore, the higher proportion of TSAP isomer observed for some of these complexes, may allow improved relaxometric properties.

The NMRD profiles in water and in human serum at 25 °C and 37 °C (Figure 4A and S20) and the variable-temperature $^{17}\text{O-NMR}$ R_2 profiles (Figure 4B and S22), were measured in order to define

FULL PAPER

the determinants of the relaxometric properties of the investigated complexes.

In human serum, the NMRD profiles of Gd-HIBDO3A and Gd-HMPDO3A both indicate a small 'hump' in the high field region (10 – 100 MHz, Figure 4A.i.), which is not observable for Gd-HPDO3A and Gd-HEDO3A. An increase in relaxivity in the high-field region is indicative of binding interactions with macromolecules and therefore a slow tumbling time (τ_R). To gain more insight into the observed behaviour, the NMRD profile of Gd-HMPDO3A with human serum albumin (HSA, 35 mg/ml) was also measured. However, it did not display any increase in relaxivity in the high-field region (Figure S21). This has previously been observed for the complex Gd-PhenDO3A, that has a phenyl substituent instead of a methyl group, which demonstrated a larger 'hump' than the complexes described here but had no such interaction with HSA.^[26] It is possible that hydrophobic interactions with another undetermined protein in serum result in a reduction in molecular tumbling time yielding the small increase in relaxivity in this region. Though small, this effect indicates how minor structural modifications may control specific interactions with blood serum components and outlines the high detection sensitivity of the relaxometric measurements through the complex interplay between τ_R , τ_m and the other parameters.

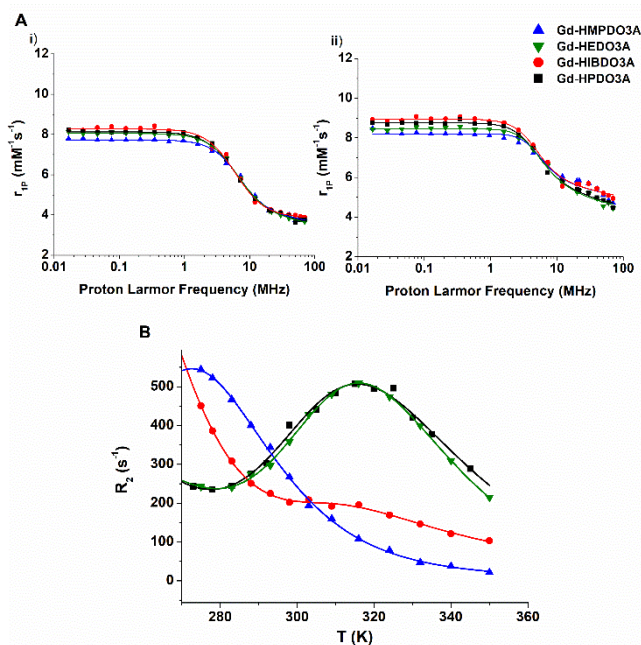


Figure 4. A) NMRD profiles in i) water and ii) human serum measured at 298 K. B) ^{17}O -NMR profiles measured at variable temperature and 600 MHz, of 20 mM Gd complex in H_2O . Gd complexes measured in A and B are: Gd-HMPDO3A (blue), Gd-HEDO3A (green) and Gd-HIBDO3A (red), compared to Gd-HPDO3A (black), at pH 7.

The NMRD and ^{17}O -NMR data were analysed independently using the Swift-Connick theory for ^{17}O relaxation, and the Solomon-Bloembergen-Morgan (SBM) and Freed's model for inner- and outer-sphere proton relaxation.^[27] A two-isomer model was used in the fitting of the ^{17}O -NMR data for Gd-HMPDO3A and Gd-HEDO3A, where the ratio of isomers in the Gd complexes was extrapolated from the corresponding Eu complexes. In analogy with what has been previously reported,^[20,28] we considered that it was reasonable to assume the SAP/TSAP ratios for Gd-

complexes are not too far from those of the corresponding Eu-complexes and comparable with what was observed for Eu- and Gd-HPDO3A (i.e. $\chi_{\text{SAP}}(\text{Gd}) = \chi_{\text{SAP}}(\text{Eu}) \times 1.16$; $\chi_{\text{TSAP}}(\text{Gd}) = 100 - \chi_{\text{SAP}}(\text{Gd})$, Table 1). A single isomer model was used for the fitting of Gd-HIBDO3A ^{17}O -NMR data, as it was found that the low calculated proportion of SAP isomer in the Gd complex (0.06) made the two-isomer fitting model unreliable.

The parameters determined from fitting the ^{17}O -NMR and NMRD data are displayed in Table 2. The values of the exchange lifetime (τ_m) and activation energy for water exchange (ΔH_m) were derived from the fitting of the ^{17}O -NMR data. The derived weighted average of τ_m for the two isomers was then fixed in the fitting of the NMRD data and the rotational correlation time (τ_R), squared mean transient zero-field splitting energy (Δ^2) and electronic relaxation time (τ_V) determined. These values are comparable across the complexes to those of Gd-HPDO3A, while the τ_m values differ markedly. Whereas Gd-HEDO3A and Gd-HPDO3A display very similar τ_m values, Gd-HMPDO3A and Gd-HIBDO3A have significantly shorter average water exchange lifetimes. For Gd-HMPDO3A, the τ_m value of the TSAP isomer is comparable to that of Gd-HPDO3A, while that of the SAP isomer is significantly shorter (around 26 times shorter). As the TSAP isomer is almost exclusively present in Gd-HIBDO3A, the complex displays a short water exchange lifetime (average τ_m ca. 16 ns). The average water exchange lifetimes of both Gd-HIBDO3A and Gd-HMPDO3A are close to what has been determined the optimal range for proton relaxation enhancers at clinical imaging fields (24 ns).

Table 2. Fitting parameters from analysis of ^{17}O -NMR and ^1H -NMRD^[a] profiles for Gd-HPDO3A derivatives.

Parameters	Gd-HPDO3A ^[b]	Gd-HEDO3A ^[c]	Gd-HIBDO3A ^[d]	Gd-HMPDO3A ^[c]
Mol.Frac ⁿ TSAP	0.3	0.4	-	0.4
$^{298}r_{1p}$ water ^[e]	4.2	4.2	4.3	4.3
$^{298}r_{1p}$ serum ^[e]	5.4	5.3	5.7	5.9
τ_m (ns) SAP	640	546.3 ± 25.7	16.1 ± 2.8	24.4 ± 3.9
TSAP	8.9	6.6 ± 2.7		7.0 ± 2.9
Weighted avg. τ_m (ns)	451	330	16.1	17.4
ΔH_m ^[f] SAP	53	54.8 ± 2.5	19.5 ± 3.2	61.6 ± 9.9
TSAP	15	43.3 ± 13.2		27.8 ± 8.3
τ_R (ps)	65	54.2 ± 1.0	62.1 ± 2.7	56.0 ± 0.1
Δ^2 (10^{19} s^{-2})	7.4	2.7 ± 0.2	5.4 ± 1.0	3.7 ± 0.1
τ_V (ps)	14.6	21.3 ± 1.6	12.9 ± 1.8	20.7 ± 0.1

[a] a NMRD profiles used for fitting were acquired at 298 K in water, with the following parameters fixed during the fitting procedure: $q = 1$, $r_{\text{GdH}} = 3.1 \text{ \AA}$, $a_{\text{GdH}} = 3.8 \text{ \AA}$, $D_{\text{GdH}} = 2.24 \times 10^{-5} \text{ cm}^2 \text{ s}^{-1}$. [b] From ref.^[12] [c] Two-isomer model was used for fitting of the ^{17}O -NMR data with fixed parameters: $r_{\text{GdO}} = 2.5 \text{ \AA}$, $E_r = 10 \text{ kJmol}^{-1}$, $E_v = 10 \text{ kJmol}^{-1}$, $A/\hbar = -3.5 \times 10^6 \text{ rad s}^{-1}$, $\tau_{\text{R0}} = 90 \text{ ps}$. [d] Single isomer model used for fitting of Gd-HIBDO3A ^{17}O -NMR data with the same fixed parameters as the two isomer model except $E_r = 20 \text{ kJmol}^{-1}$ and E_v was left unfixed. [e] $\text{mM}^{-1} \text{ s}^{-1}$. [f] kJmol^{-1} .

FULL PAPER

The remarkably short exchange lifetime of the coordinated water molecule in Gd-HMPDO3A parallels well with previously reported results obtained on macrocyclic complexes containing an elongated carboxo-amide arm. In fact, Toth and co-workers showed that the increased steric crowding at the water coordination site, obtained by replacing an ethylene bridge of DOTA⁴⁻ by a propylene bridge, resulted in a dramatic increase of the water exchange rate.^[29]

Prototropic exchange

The relaxivity of Gd-HPDO3A has been previously shown to be markedly pH dependent, with a significant increase in relaxivity at high pH values (> 8 – 10.4) as a result of base catalysed exchange of the hydroxyl proton.^[30] The pK_a of the hydroxyl proton in Gd-HPDO3A is 11.36,^[31] and therefore the decrease in relaxivity above pH 10.4 was attributed to the formation of the deprotonated anionic complex.^[30] Similar behaviour is observed for the Gd-HPDO3A derivatives (Figure 5). Gd-HEDO3A remained the most similar to Gd-HPDO3A, as it exhibited an increase of 1.3 mM⁻¹s⁻¹ at pH 10.6 compared to 1.4 mM⁻¹s⁻¹ at pH 10.4 for Gd-HPDO3A. Gd-HIBDO3A demonstrates a maximum increase of 1.6 mM⁻¹s⁻¹ at pH 11 which is a notable enhancement in the maximum relaxivity as well as a shift towards a higher pH. The higher pH value of the maximum relaxivity enhancement is consistent with a higher pK_a of tertiary alcohols. However, the cause of the higher relaxivity enhancement is uncertain, perhaps the OH group is located closer to the Gd in this structure than the other HPDO3A derivatives, or the exchange of the hydroxyl proton is faster.

Gd-HMPDO3A shows a distinct lower enhancement of the relaxivity with increasing pH. The complex displays a maximum enhancement of 0.8 mM⁻¹s⁻¹ at pH 9.8. The shift in pH is again consistent with the lower pK_a of primary alcohols, while the lower enhancement is most likely the result of the increased Gd-H distance in Gd-HMPDO3A compared to Gd-HPDO3A. An increase of 0.8 mM⁻¹s⁻¹ corresponds to the exchange of one proton at a Gd-H distance of 3.3 Å, in comparison to 3 Å in Gd-HPDO3A.^[30]

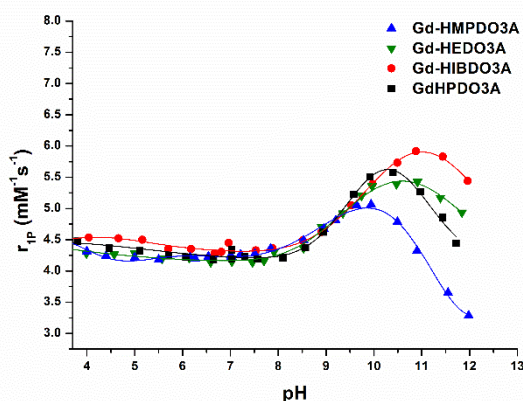


Figure 5. Relaxivity of Gd-HPDO3A derivatives versus pH measured at 298 K and 0.47 T. Symbols indicate experimental data, solid lines are drawn freehand to aid visualisation of the data.

Stability and Anion Binding

The Gd complexes were tested for their kinetic stability by measuring the rate of transmetalation with zinc chloride in phosphate buffer.^[32] Gd-HEDO3A and Gd-HIBDO3A maintain the same kinetic stability as Gd-HPDO3A as they display no evidence of transmetalation with zinc over the time course of the experiment (Figure 6). However, Gd-HMPDO3A displays a reduction in kinetic stability as zinc is able to displace Gd from the complex with approximately a 25 % displacement over 3 days. This is due to the elongation of the hydroxypropyl arm, which reduces the stability of the coordinating hydroxyl group as it is located further from the gadolinium centre than in the prior Gd-HPDO3A complexes. Gd-HPDO3A appears to show a small increase in the relaxivity after 4 days, which was not observed in the data recorded by Laurent *et al.* as they did not record beyond this time point.^[32] The reason for this increase is unclear, but as it is known that phosphate can enhance the second sphere relaxation contribution, perhaps there is some slow coordination of zinc and phosphate to the ligand sphere of Gd-HPDO3A that increases the observed relaxation rate over time.^[33]

The rate of transmetalation of Gd-HMPDO3A with zinc is slower than that reported for any of the linear chelates. After 3 days, $R_{1P}(t)/R_{1P}(t=0)$ is 0.76 for Gd-HMPDO3A while for all linear chelates it was reported to be below 0.7. In addition to this, the linear chelates show a quicker initial decrease over the first couple of days, as the data shows it takes Gd-HMPDO3A 3650 min to reach $R_{1P}/R_{1P}(t=0) = 0.8$, while for the linear chelates it takes between 1500 min (Gd-EOB-DTPA) and 70 min (Gd-DTPA-BMA).^[32] Thus, these results suggest that the stability of Gd-HMPDO3A is not low enough to prevent *in vivo* studies, given the improvement over linear agents.

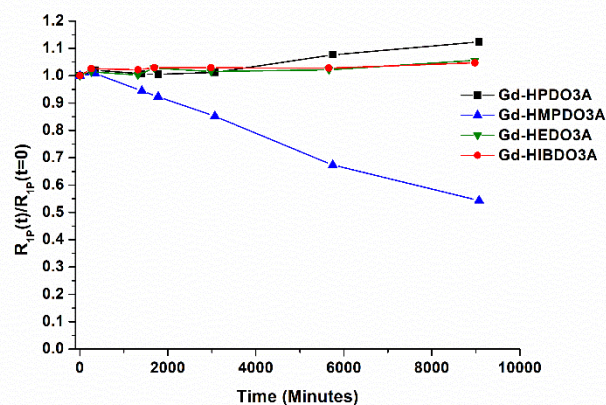


Figure 6. Zinc transmetalation as modelled by the change in $R_{1P}(t)/R_{1P}(t=0)$ over time for the different Gd-HPDO3A derivatives at 310 K.

The reduced strength of the coordinating hydroxyl group in Gd-HMPDO3A allows some displacement by strongly coordinating bidentate anions such as lactate. The complexes were tested for their interaction with phosphate (Na_2HPO_4), Carbonate (NaHCO_3), citrate and lactate in 150 mM NaCl, 10 mM HEPES buffer. In the presence of 50 mM lactate the relaxivity of Gd-HMPDO3A is reduced from 4.45 mM⁻¹s⁻¹ (r_{1P} in NaCl/HEPES) to 3.6 mM⁻¹s⁻¹ – a 19 % decrease, while with carbonate, citrate and phosphate the relaxivity remains comparable. (Figure S23) At more basic pH values (pH 8) it was found that some binding of carbonate does

FULL PAPER

occur. The other complexes, including Gd-HPDO3A, do not show significant changes in relaxivity even with high concentrations (50 mM) of these anions.

Conclusion

Three ligands have been synthesised and investigated for their relaxometric properties relating to the hydroxylpropyl moiety. In particular, it was found that increasing the distance of the hydroxyl group from the lanthanide centre by one carbon group (HMPDO3A) enhanced the water exchange dynamics of the complex, but at the expense of decreasing kinetic stability. Removal of the methyl group in HPDO3A to give HEDO3A was shown to have little effect on the properties of the Gd complex, both in the water exchange dynamics and also in the overall observed relaxivity. Meanwhile, Gd-HIBDO3A demonstrated significant differences to Gd-HPDO3A in terms of water exchange and the ratio of isomers that results from the addition of one methyl group. The observed relaxivity profiles remain relatively unchanged since the molecular tumbling time limits the achievable enhancement of relaxivity beyond water exchange rates. With a larger molecular weight and slower rotational correlation time it is expected that higher relaxivity values could be achieved. Overall, Gd-HIBDO3A maintains all the benefits of Gd-HPDO3A while increasing the rate of water exchange to give a τ_m value within the optimal range.^[34] These results demonstrate how small modifications to the hydroxyl group in HPDO3A allow significant alterations to the observed properties of the lanthanide complexes. Understanding how this clinical probe can be adapted to further enhance or modify its application in MRI and CEST provides a useful insight for the future development of high relaxation enhancers or reporter probes.

Experimental Section

General: All chemicals were purchased from Sigma-Aldrich Co. and were used without purification. 1,4,7,10-tetraazacyclododecane-1,4,7-triacetic acid 1,4,7-tris(1,1-dimethylethyl) ester (1) was synthesized according to literature procedures.^[18] Mass spectra were recorded on a Waters Acquity UPLC H class coupled with QDa detector mass spectrometer (direct infusion with H₂O 0.1% COOH (or TFA)/ACN 0.1% COOH (or TFA) 50:50). pH measurements were made using an AS instruments pH meter equipped with a glass electrode. Chromatographic purification was performed using an AKTA Purifier equipped with a UV-900 system, P-900 pump, frac-920 fraction collector and an Amberchrom® CG161 resin column. ¹H-NMR spectra were acquired at 14.1 T on a Bruker Avance 600 spectrometer equipped with a 5 mm probe and standard temperature control unit.

Synthesis: 2-(2-bromoethoxy)tetrahydro-2H-pyran (2). A solution of 2-bromoethanol (40.5 g; 23 ml; 0.33 mol) and pyridinium p-toluenesulfonate (8.3 g; 33 mmol) in DCM (150 ml) was cooled with an ice bath and 3,4-dihydropyran (41.6 g; 45 ml; 0.5 mol) in DCM (50 ml) was slowly added. After one night at room temperature, the mixture was washed with water (3 x 100ml) and brine (100 ml), dried over Na₂SO₄ and distilled: the 2-(2-

bromoethoxy)tetrahydro-2H-pyran boils at 85°C and 147 mbar (29.2 g).

1,4,7,10-tetraazacyclododecane-10-(2-((tetrahydro-2H-pyran-2-yl)oxy)ethyl)-1,4,7-triacetic acid 1,4,7 tri-tert-butyl ester (3). To a solution of 1,4,7,10-tetraazacyclododecane-1,4,7-triacetic acid 1,4,7-tris(1,1-dimethylethyl) ester hydrobromide (1) (15 g; 25 mmol) in 150 ml of ACN, K₂CO₃ (-325 mesh, 10.4 g; 75 mmol) and 2-(2-bromoethoxy)tetrahydropyran (2) (5.75 g; 342 μl; 27.5 mmol) in 50 ml of ACN were added. After one night the mixture was filtered and evaporated. The residue was dissolved in ethyl acetate (100 ml) and washed with water (2 x 25 ml) and brine (15 x 20 ml) to obtain the substitution of bromide with chloride, then evaporated (15 g).

1,4,7,10-tetraazacyclododecane-10-(2-hydroxy-ethyl)-1,4,7-triacetic acid (4, HEDO3A) The 1,4,7,10-tetraazacyclododecane-10-(2-((tetrahydro-2H-pyran-2-yl)oxy)ethyl)-1,4,7-triacetic acid 1,4,7 tri-tert-butyl ester (3) was dissolved in water (30 ml), THF (60 ml) and Acetic Acid (120 ml) and stirred at room temperature; after 24 hours the mixture was evaporated to give a residue. Cooling with an ice bath, the product was dissolved in TFA (40 ml) with 2 drops of Triisopropylsilane and stirred at room temperature for 3 days. The product was precipitated with diethyl ether, filtered and dried under vacuum. The crude product was purified by chromatography on an Amberchrom CG161 resin (eluent: 0.2% TFA in water). The fraction containing the pure product was freeze dried. (8.3 g). HCl 1N (60 ml) was added and the solution was stirred for 1 hour, then freeze dried (7.3 g of 1,4,7,10-tetraazacyclododecane-10-(2-hydroxy-ethyl)-1,4,7-triacetic acid tetrahydrochloride). ¹H-NMR (600 MHz, D₂O): δ_H = 4.14 (s, 2 H, -CH₂COO), 3.99 (t, 2 H, -CH₂OH), 3.63-3.09 (m, 22 H, -NCH₂). ¹³C-NMR (150 MHz, D₂O): δ_C = 173.4 (-COO), 168.3 (-COO), 54.7 (-CH₂OH), 54.3(-CH₂COO), 54.2 (-CH₂CH₂OH) 52.2 (-CH₂COO), 51.0, 49.8, 47.5, 47.2 (CH₂ cyclen ring) ppm. MS ESI: *m/z* calcd 391.22 [M+H]⁺; found 391.33.

1,4,7,10-tetraazacyclododecane-10-(2-hydroxy-2-methylpropyl)-1,4,7-triacetic acid 1,4,7 tri-tert-butyl ester (5).

To a solution of 1,4,7,10-tetraazacyclododecane-1,4,7-triacetic acid 1,4,7-tris(1,1-dimethylethyl) ester (1) (20 g; 38.8 mmol) and DIPEA (15 g; 20.3 ml; 116.5 mmol) in 100 ml of ACN, 1,2-Epoxy-2-methylpropane (4.2 g; 5.2 ml; 58.3 mmol) was added. The reaction was monitored by TLC (eluent DCM/MeOH 1:1, stain KMnO₄): after 2 days at 50°C the mixture was evaporated and redissolved in ethyl acetate (200 ml), washed with water (5 x 30 ml), dried over Na₂SO₄ and evaporated to residue (19.7 g).

1,4,7,10-tetraazacyclododecane-10-(2-hydroxy-2-methylpropyl)-1,4,7-triacetic acid (6, HIBDO3A). The crude 1,4,7,10-tetraazacyclododecane-10-(2-hydroxy-2-methylpropyl)-1,4,7-triacetic acid 1,4,7 tri-tert-butyl ester (5) (19.7 g; 33,6 mmol) was dissolved in DCM (50 ml), acidified with TFA (10 ml), evaporated and dissolved in TFA (50 ml) with triisopropylsilane (2 drops). After one night the TFA was evaporated and replaced: after 2 days the deprotection was complete and the product was precipitated with diethyl ether, filtered and dried under vacuum. The crude product was purified by chromatography on an Amberchrom CG161 resin (eluent: water/MeOH gradient). The fraction containing the pure product was evaporated and freeze dried. (4.8 g). ¹H-NMR (600 MHz, D₂O): δ_H = 4.06 (s, 2 H, CH₂COO), 3.93 (d, 2 H, CH₂COO), 3.63-3.09 (m, 18 H, CH₂), 3.39 (s, 2H, -CH₂C(CH₃)₂OH), 1.36 (s, 6 H, CH₃) ppm. ¹³C-NMR (150

FULL PAPER

MHz, D₂O): δ_C = 173.2 (-COO), 168.6 (-COO), 67.7 (-C(CH₃)₂OH), 62.7 (-CH₂C(CH₃)₂OH), 54.7 (-CH₂COO), 52.6 (CH₂COO), 52.3, 50.6, 47.5, 46.6 (CH₂ cyclen ring), 26.6 (-CH₃) ppm. MS ESI *m/z* calcd 419.25 [M+H⁺]; found 418.95.

1,4,7,10-tetraazacyclododecane-10-(3-hydroxy-2-methylpropyl)-1,4,7-triacetic acid 1,4,7 tri-*tert*-butyl ester (7).

To a solution of 1,4,7,10-tetraazacyclododecane-1,4,7-triacetic acid 1,4,7-tris(1,1-dimethylethyl) ester hydrobromide (1) (1.5 g; 2.5 mmol) in 25 ml of ACN, K₂CO₃ (-325 mesh, 1.4 g; 10 mmol) and 3-bromo-2-methyl-1-propanol (0.5 g; 342 μ l; 3.2 mmol) dissolved in 5 ml of ACN were added. The reaction was monitored by MS ESI+. The mixture was filtered and evaporated to residue (1 g).

1,4,7,10-tetraazacyclododecane-10-(3-hydroxy-2-methylpropyl)-1,4,7-triacetic acid. (8, HMPDO3A) The crude 10-[2-methyl-3-hydroxypropyl]-1,4,7,10-tetraazacyclododecane-1,4,7-triacetic acid 1,4,7-tris(1,1-dimethylethyl) ester (7) was dissolved in DCM (15 ml), acidified with TFA (3 ml), then evaporated and dissolved in TFA (15 ml) with triisopropylsilane (2 drops). After one night the TFA was evaporated and replaced: after 2 days the deprotection was complete and the product was precipitated with diethyl ether, filtered and dried under vacuum. The crude product was purified by chromatography on an Amberchrom CG161 resin (eluent: water). The fraction containing the pure product was freeze dried. (450 mg). ¹H-NMR (600 MHz, D₂O): δ_H = 4.04-2.93 (m, 26 H, CH₂ cyclen ring and pendant arms), 2.43 (br, 1 H, -CHCH₃CH₂OH), 0.94 (d, 3 H, CH₃). ¹³C-NMR (150 MHz, D₂O): δ_C = 173.5 (-COO), 173.1 (-COO), 169.4 (-COO), 66.2 (-CH₂OH), 60.0 (-NCH₂CH-), 55.9 (-CH₂COO), 52.1 (-CH₂COO), 52.0 (-CH₂COO), 51.6, 50.8, 49.8, 49.1, 48.5, 48.0, 46.0, 44.5 (CH₂ cyclen ring), 28.5 (-CHCH₃), 12.7 (-CH₃) ppm. MS ESI: *m/z* calcd 419.25 [M+H⁺]; found 419.32.

Complexation with Ln(III): A similar method to the following procedure was used for all lanthanide complexations. Characterisation data for all complexes are listed. The isotope patterns in the mass spec data were consistent with Eu(III) and Gd(III). Only fully resolved peaks are reported for ¹H-NMR recorded at 275 K.

Gd-HEDO3A The 1,4,7,10-tetraazacyclododecane-10-(2-hydroxy-ethyl)-1,4,7-triacetic acid tetrahydrochloride (4) (150 mg; 0.3 mmol) was dissolved in water (10 ml) and basified to pH 7 with NaOH 0.1N. A solution of GdCl₃ in water was gradually added, while maintaining pH 7 with NaOH 0.1N, until the presence of residual free Gd³⁺ in the solution was confirmed by the orange xylenol UV method.^[35] The product was purified by chromatography on an Amberchrom CG161 resin (eluent: water/ACN gradient). The fraction containing the pure product was evaporated and freeze dried. (97 mg). MS ESI: *m/z* calcd 546.12 [M+H⁺]; found 546.05.

Eu-HEDO3A ¹H-NMR (600 MHz, D₂O): δ_H = 35.66, 34.90, 29.86, 24.71, 13.33, 11.37, 10.57, 7.55, 5.49, 3.98, 3.34, 2.05, 1.34, 0.39, -0.83, -1.96, -2.44, -3.57, -4.52, -6.06, -7.49, -8.19, -9.07, -9.79, -10.58, -11.31, -11.97, -14.54, -15.37, -16.06, -17.35, -19.02, -21.30 ppm. MS ESI: *m/z* calcd 541.12 [M+H⁺]; found 541.21.

Gd-HIBDO3A MS ESI: *m/z* calcd 574.15 [M+H⁺]; found 574.24.

Eu-HIBDO3A ¹H-NMR (600 MHz, D₂O): δ_H = 15.36, 12.59, 12.17, 10.87, 6.60, 3.99, 3.52, 2.33, 0.19, -1.51, -4.17, -6.16, -6.72, -7.16, -8.77, -11.18, -12.21, -13.05, -16.05 ppm. MS ESI: *m/z* calcd 569.15 [M+H⁺]; found 569.21.

Gd-HMPDO3A MS ESI: *m/z* calcd 574.15 [M+H⁺]; found 574.24.

Eu-HMPDO3A ¹H-NMR (600 MHz, D₂O): δ_H = 38.95, 33.92, 33.69, 32.87, 32.44, 31.53, 27.39, 22.44, 15.86, 13.93, 13.37, 12.99, 11.34, 10.39, 9.03, 5.64, 5.42, 3.39, 1.77, 1.07, 0.94, 0.58, -1.11, -1.31, -2.03, -4.08, -4.71, -5.49, -6.17, -6.62, -7.16, -7.34, -7.60, -7.71, -8.31, -8.79, -9.29, -9.58, -9.70, -11.07, -11.45, -11.84, -12.07, -12.44, -13.50, -14.44, -14.67, -18.46, 19.43, -20.48, -20.74, -21.05, -21.24, -22.12, -24.32 ppm. MS ESI: *m/z* calcd 569.15 [M+H⁺]; found 569.27.

High Resolution ¹H-NMR: For high resolution ¹H-NMR of europium complexes, samples were dissolved in D₂O at ca. 100 mM concentration and the pH adjusted with NaOD or DCI to 7 (pD = 7.4). The temperature was varied from 275 to 350 K according to the experiments. EXSY experiments were acquired using the standard NOESY pulse sequence (90°-t₁-90°-T_M-90°) with the mixing time (T_M) set to 5 ms unless otherwise stated.

Relaxometric Measurements: R_{1obs} values were determined by inversion recovery at 21.5 MHz and 25 °C using a Stelar SpinMaster spectrometer (Stelar Snc, Meade (PV), Italy). Temperature was controlled with a Stelar VTC-91 airflow heater and the temperature inside the probe checked with a calibrated RS PRO RS55-11 digital thermometer. Data was acquired using a recovery time $\geq 5 \times T_1$ and with 2 scans per data point. The absolute error in R₁ measurements was less than 1 %.

The gadolinium concentration of the complexes was determined using the previously described relaxometric technique.^[36] Briefly, gadolinium complex solutions were mixed in equal volumes with 37 % HCl and heated in sealed vials at 120 °C overnight to solubilize the free Gd³⁺ aqua ion. The R₁ of the solution was measured at 25 °C and 21.5 MHz and the concentration determined using the equation: $R_{1obs} = R_{1d} + r_{1P}^{Gd} [Gd]$. Where R_{1d} is the diamagnetic contribution (0.5 s⁻¹) and r_{1P}^{Gd} is the relaxivity (13.5 mM⁻¹s⁻¹) under the same experimental conditions.

Transmetallation experiments were performed as follows: Gd complexes were dissolved in phosphate buffer (26 mM KH₂PO₄ and 41 mM Na₂HPO₄) at pH 7. ZnCl₂ solution (250 mM ZnCl₂ in H₂O) was added to give an equimolar Gd : Zn solution. Two samples were measured for each complex and the average of R_{1obs} taken. The relaxation rate of the solution at 298 K, 21 MHz was measured (t=0) the tubes were kept at 310 K and subsequent measurements were taken over the course of a week.

Anion interaction was determined by measurement of the relaxation rate at 298 K and 21 MHz in 10 mM HEPES with 150 mM NaCl at pH 7.4, with addition of a known concentration of anion (0-50 mM).

NMRD and ¹⁷O-NMR: NMRD profiles were obtained using a Stelar SpinMaster FFC NMR relaxometer from 0.01 – 20 MHz and a Bruker WP80 NMR electromagnet for variable higher-field measurements (21.5 – 70 MHz), both equipped with a Stelar VTC-91 for temperature control. Aqueous and human serum solutions of the Gd complexes ([Gd] = 0.5 - 1.5 mM) were measured at 298 K and 310 K.

For ¹⁷O-NMR measurements, 10 mM Gd solutions of the complexes in H₂O with 1% H₂¹⁷O isotope (Cambridge Isotope) were made with capillary inserts of D₂O and measured on a Bruker Avance 600 MHz spectrometer with temperature control. The full width at half maximum ($\Delta\omega$) was used to calculate the

FULL PAPER

observed transverse relaxation rate using the equation: $R_2 = \pi[\Delta\omega_{\text{obs}} - \Delta\omega_{\text{H}_2\text{O}}]$.

The NMRD profiles data and ^{17}O -NMR data were analysed independently and fitted using the SBM and Freed's model, and Swift-Connick equations respectively. A single or two isomer model was used to fit the ^{17}O -NMR profiles and the weighted average of the exchange lifetimes (τ_M) were fixed as parameters for the NMRD fitting procedures.

Acknowledgements

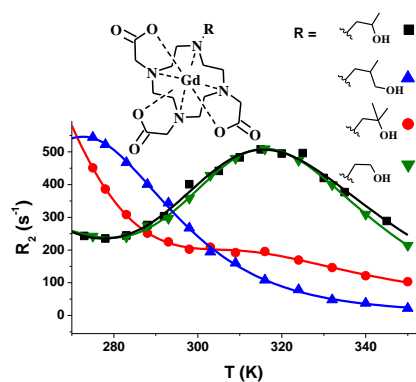
This work has received funding from Regione Piemonte (P.O.R. FESR 2014/2020 Bando IR2 – Industrializzazione dei risultati della ricerca - project "Gadoplus") and it was performed in the framework of COST Action AC15209 (EURELAX).

Keywords: gadolinium • MRI contrast agents • lanthanides • macrocycles • relaxometry

- [1] L. M. De León-Rodríguez, A. F. Martins, M. C. Pinho, N. M. Rofsky, A. D. Sherry, *J. Magn. Reson. Imaging* **2015**, *42*, 545–65.
- [2] D. D. Dischino, E. J. Delaney, J. E. Emswiler, G. T. Gaughan, J. S. Prasad, S. K. Srivastava, M. F. Tweedle, *Inorg. Chem* **1991**, *30*, 1265–1269.
- [3] T. Kanda, K. Ishii, H. Kawaguchi, K. Kitajima, D. Takenaka, *Radiology* **2014**, *270*, 834–841.
- [4] R. J. McDonald, J. S. McDonald, D. F. Kallmes, M. E. Jentoft, D. L. Murray, K. R. Thielen, E. E. Williamson, L. J. Eckel, *Radiology* **2015**, *275*, 772–782.
- [5] N. Murata, L. F. Gonzalez-Cuyar, K. Murata, C. Fligner, R. Dills, D. Hippe, K. R. Maravilla, *Invest. Radiol.* **2016**, *51*, 447–453.
- [6] R. J. McDonald, D. Levine, J. Weinreb, E. Kanal, M. S. Davenport, J. H. Ellis, P. M. Jacobs, R. E. Lenkinski, K. R. Maravilla, M. R. Prince, et al., *Radiology* **2018**, *289*, 517–534.
- [7] G. Jost, T. Frenzel, J. Boyken, J. Lohrke, V. Nischwitz, H. Pietsch, *Radiology* **2019**, *290*, 340–348.
- [8] S. Bussi, A. Coppo, C. Botteron, V. Fraimbault, A. Fanizzi, E. De Laurentiis, S. Colombo Serra, M. A. Kirchin, F. Tedoldi, F. Maisano, *J. Magn. Reson. Imaging* **2018**, *47*, 746–752.
- [9] R. J. McDonald, J. S. McDonald, D. Dai, D. Schroeder, M. E. Jentoft, D. L. Murray, R. Kadirvel, L. J. Eckel, D. F. Kallmes, *Radiology* **2017**, *285*, 536–545.
- [10] T. Frenzel, P. Lengsfeld, H. Schirmer, J. Hütter, H. J. Weinmann, *Invest. Radiol.* **2008**, *43*, 817–828.
- [11] J. M. Idée, M. Port, C. Robic, C. Medina, M. Sabatou, C. Corot, *J. Magn. Reson. Imaging* **2009**, *30*, 1249–1258.
- [12] D. Delli Castelli, M. C. Caligara, M. Botta, E. Terreno, S. Aime, *Inorg. Chem.* **2013**, *52*, 7130–7138.
- [13] K. Kumar, C. A. Chang, L. C. Francesconi, D. D. Dischino, M. F. Malley, J. Z. Gougoutas, M. F. Tweedle, *Inorg. Chem.* **1994**, *33*, 3567–3575.
- [14] S. Aime, S. Baroni, D. Delli Castelli, E. Brücher, I. Fábíán, S. C. Serra, A. Fringuello Mingo, R. Napolitano, L. Lattuada, F. Tedoldi, et al., *Inorg. Chem.* **2018**, *57*, 5567–5574.
- [15] F. A. Dunand, R. S. Dickins, D. Parker, A. E. Merbach, *Chem. - A Eur. J.* **2001**, *7*, 5160–5167.
- [16] G. Ferrauto, D. D. Castelli, E. Terreno, S. Aime, *Magn. Reson. Med.* **2013**, *69*, 1703–1711.
- [17] D. Delli castelli, E. Terreno, S. Aime, *Angew. Chemie - Int. Ed.* **2011**, *50*, 1798–1800.
- [18] H. Oskar Axelsson, M. Andreas Olsson, *Synthesis of Cyclen Derivatives*, **2006**, WO 2006/112723.
- [19] K. Kumar, T. Jin, X. Wang, J. F. Desreux, M. F. Tweedle, *Inorg. Chem* **1994**, *33*, 3823–3829.
- [20] G. Ferrauto, D. Delli Castelli, L. Leone, M. Botta, S. Aime, Z. Baranyai, L. Tei, *Chem. - A Eur. J.* **2019**, *25*, 4184–4193.
- [21] S. Aime, M. Botta, G. Ermondi, *Inorg. Chem* **1992**, *31*, 4291–4299.
- [22] T. J. Clough, L. Jiang, K.-L. Wong, N. J. Long, *Nat. Commun.* **2019**, *10*, 1420.
- [23] L. Dai, C. M. Jones, W. T. K. Chan, T. A. Pham, X. Ling, E. M. Gale, N. J. Rotile, W. C. S. Tai, C. J. Anderson, P. Caravan, et al., *Nat. Commun.* **2018**, *9*, 1–10.
- [24] G. Tircso, B. C. Webber, B. E. Kucera, V. G. Young, M. Woods, *Inorg. Chem.* **2011**, *50*, 7966–7979.
- [25] S. Aime, M. Botta, Z. Garda, B. E. Kucera, G. Tircso, V. G. Young, M. Woods, *Inorg. Chem.* **2011**, *50*, 7955–7965.
- [26] A. Fringuello Mingo, S. Colombo Serra, S. Baroni, C. Cabella, R. Napolitano, I. Hawala, I. M. Carnovale, L. Lattuada, F. Tedoldi, S. Aime, *Magn. Reson. Med.* **2017**, *78*, 1523–1532.
- [27] L. Leone, G. Ferrauto, M. Cossi, M. Botta, L. Tei, *Front. Chem.* **2018**, *6*.
- [28] L. Leone, D. Esteban-Gómez, C. Platas-Iglesias, M. Milanésio, L. Tei, *Chem. Commun.* **2019**, *55*, 513–516.
- [29] R. Ruloff, É. Tóth, R. Scopelliti, R. Tripier, H. Handel, A. E. Merbach, *Chem. Commun.* **2002**, *2*, 2630–2631.
- [30] S. Aime, M. Botta, M. Fasano, E. Terreno, *Acc. Chem. Res.* **1999**, *32*, 941–949.
- [31] É. Tóth, R. Király, J. Platzek, B. Radüchel, E. Brücher, *Inorganica Chim. Acta* **1996**, *249*, 191–199.
- [32] S. Laurent, L. Vander Elst, C. Henoumont, R. N. Muller, *Contrast Media Mol. Imaging* **2010**, *5*, 305–308.
- [33] M. Botta, S. Aime, A. Barge, G. Bobba, R. S. Dickins, D. Parker, E. Terreno, *Chem. Eur. J.* **2003**, *9*, 2102–2109.
- [34] A. D. Sherry, Y. Wu, *Curr. Opin. Chem. Biol.* **2013**, *17*, 167–174.
- [35] A. Barge, G. Cravotto, E. Gianolio, F. Fedeli, *Contrast Media Mol. Imaging* **2006**, *1*, 184–188.
- [36] E. Gianolio, C. Cabella, S. Colombo Serra, G. Valbusa, F. Arena, A. Maiocchi, L. Miragoli, F. Tedoldi, F. Uggeri, M. Visigalli, et al., *J. Biol. Inorg. Chem.* **2014**, *19*, 715–726.

FULL PAPER

Entry for the Table of Contents



The hydroxyl arm of Gd-HPDO3A has been modified to form three derivatives, which have been fully analysed for their relaxometric properties. It was found that these small modifications could significantly alter the proportion of isomers and increase the water exchange rate through minor adjustments to the hydroxyl group environment. In particular, increasing the steric bulk around the OH group allowed the properties of Gd-HPDO3A to be optimised.